2013

Cone phosphodiesterase-6α′ restores rod function and confers distinct physiological properties in the rod phosphodiesterase-6β-deficient rd10 mouse

Wen-Tao Deng
University of Florida

Keisuke Sakurai
Washington University School of Medicine in St. Louis

Saravanan Kolandaivelu
West Virginia University

Alexander V. Kolesnikov
Washington University School of Medicine in St. Louis

Astra Dinculescu
University of Florida

See next page for additional authors

Cellular/Molecular

Cone Phosphodiesterase-6α′ Restores Rod Function and Confers Distinct Physiological Properties in the Rod Phosphodiesterase-6β-Deficient *rd10* Mouse

Wen-Tao Deng,[1] Keisuke Sakurai,[2] Saravanan Kolandaivelu,[3] Alexander V. Kolesnikov,[2] Astra Dinculescu,[1] Jie Li,[1] Ping Zhu,[1] Xuan Liu,[4] Jijing Pang,[1] Vince A. Chiodo,[1] Sanford L. Boye,[1] Bo Chang,[5] Visvanathan Ramamurthy,[3] Vladimir J. Kefalov,[2] and William W. Hauswirth[1]

[1]Department of Ophthalmology, University of Florida, Gainesville, Florida 32610, [2]Department of Ophthalmology and Visual Sciences, Washington University School of Medicine, St. Louis, Missouri 63110, [3]Departments of Ophthalmology and Biochemistry, Center for Neuroscience, West Virginia University, Morgantown, West Virginia 26506, [4]Beijing Tsinghua Hospital, North First qu Tiantongyuan, Changping District, Beijing 102218, China, and [5]The Jackson Laboratory, Bar Harbor, Maine 04609

Phosphodiesterase-6 (PDE6) is the key effector enzyme of the vertebrate phototransduction pathway in rods and cones. Rod PDE6 catalytic core is composed of two distinct subunits, PDE6α and PDE6β, whereas two identical PDE6α′ subunits form the cone PDE6 catalytic core. It is not known whether this difference in PDE6 catalytic subunit identity contributes to the functional differences between rods and cones. To address this question, we expressed cone PDE6α′ in the photoreceptor cells of the retinal degeneration 10 (*rd10*) mouse that carries a mutation in rod PDEβ subunit. We show that adeno-associated virus-mediated subretinal delivery of PDE6α′ rescues rod electroretinogram responses and preserves retinal structure, indicating that cone PDE6α′ can couple effectively to the rod phototransduction pathway. We also show that restoration of light sensitivity in *rd10* rods is attributable to assembly of PDE6α′ with rod PDE6γ. Single-cell recordings revealed that, surprisingly, rods expressing cone PDE6α′ are twofold more sensitive to light than wild-type rods, most likely because of the slower shutoff of their light responses. Unlike in wild-type rods, the response kinetics in PDE6α′-treated *rd10* rods accelerated with increasing flash intensity, indicating a possible direct feedback modulation of cone PDE6α′ activity. Together, these results demonstrate that cone PDE6α′ can functionally substitute for rod PDEαβ *in vivo*, conferring treated rods with distinct physiological properties.

Introduction

Rod and cone photoreceptor cells share a similar phototransduction pathway but exhibit strikingly different physiological properties. Rods, responsible for scotopic vision, are highly light sensitive. Cones, responsible for photopic vision, are intrinsically less sensitive, have faster response kinetics, and adapt to a wider range of light intensities (Pugh and Cobbs, 1986; Fu and Yau, 2007). One of the key unresolved questions is how the physiological differences between rods and cones can be correlated with the distinctive properties of their phototransduction proteins. Previous studies have shown that the lower thermal stability of cone pigments is likely to contribute to the lower sensitivity of cones but, once activated, rod and cone pigments can couple equally efficiently to rod or cone transducin (Kefalov et al., 2003, 2005; Shi et al., 2005, 2007; Fu et al., 2008). Thus, consistent with our previous research (Deng et al., 2009) and other studies (Ma et al., 2001), the signaling properties of rod and cone transducin α-subunit do not contribute to the difference in light sensitivity between rods and cones (but see Chen et al., 2010). As a result, the expression levels and molecular properties of phototransduction components downstream of transducin are likely to play an important role in defining the distinctive physiological properties of rods and cones.

The photoreceptor cyclic nucleotide phosphodiesterase-6 (PDE6) plays an essential role in phototransduction by regulating the cGMP levels in rods and cones (Fu and Yau, 2007). The most obvious distinction between rod and cone PDE6 is that rod PDE6 is composed of two distinct catalytic subunits α, β (PDE6A, PDE6B) and two inhibitory subunits γ (PDE6G), whereas cone PDE6 is composed of two identical catalytic subunits α′ (PDE6C) plus two cone-specific inhibitory subunits γ′ (PDE6H) (Gillespie

Received April 10, 2013; revised May 29, 2013; accepted June 5, 2013.

Author contributions: W.-T.D., V.R., V.J.K., and W.W.H. designed research; W.-T.D., K.S., S.K., A.V.K., A.D., J.L., P.Z., X.L., J.P., V.A.C., and S.L.B. performed research; B.C. contributed unpublished reagents/analytic tools; W.-T.D., K.S., A.V.K., V.R., and V.J.K. analyzed data; W.-T.D., K.S., S.K., A.D., V.R., V.J.K., and W.W.H. wrote the paper.

W.W.H. and the University of Florida have a financial interest in the use of AAV therapies and own equity in a company (Applied Genetic Technologies, Alachua, FL) that might, in the future, commercialize some aspects of this work.

This work was supported by National Institutes of Health (NIH) Grants P30EY021721 (W.W.H.), EY019312 (V.J.K.), EY017035 (V.R.), and EY002687 (to the Department of Ophthalmology and Visual Sciences at Washington University), the Macular Vision Research Foundation, the Foundation Fighting Blindness, Research to Prevent Blindness, Inc., an Unrestricted Challenge Grant from Research to Prevent Blindness (to the Department of Ophthalmology at West Virginia University), and a Postdoctoral Scholar Award from the International Retina Research Foundation (K.S.). We thank Doug Smith, Tom Doyle, Min Ding, and Thomas Andresen for technical assistance.

Correspondence should be addressed to Wen-Tao Deng, Academic Research Building, R1-242, 1600 Southwest Archer Road, University of Florida, Gainesville, FL 32610. E-mail: wdeng@ufl.edu.

DOI: 10.1523/JNEUROSCI.1536-13.2013

 0270-6474/13/3311745-09$15.00/0

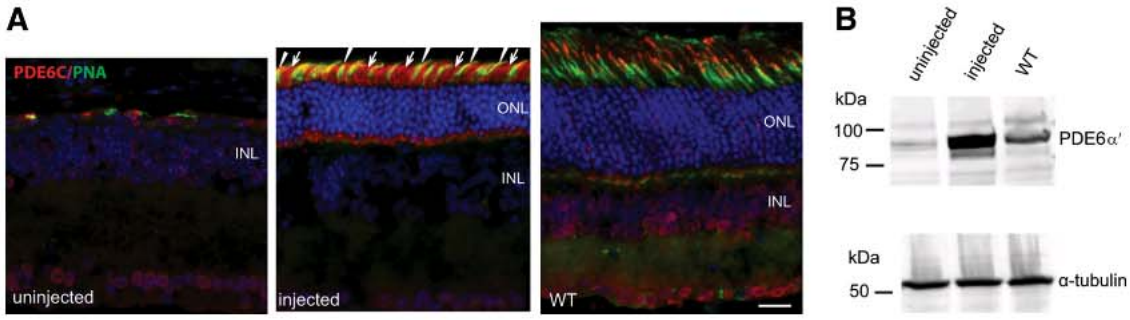

Figure 1. Detection of PDE6α′ expression after delivery of AAV8 Y733F–smCBA–PDE6α′ in *rd10* retinas. ***A***, immunofluorescence of PDE6α′ (labeled as red) expression in both rods (arrows) and cones (arrowheads) in injected retinas. PDE6α′ expression can only be detected in cones in WT control. Only spotty staining can be detected in untreated eyes because of significant retina degeneration. Cones were labeled by PNA (green). Scale bar, 20 μm. ***B***, Western blot analysis of untreated, treated *rd10*, and WT control retinas. Injected *rd10* retinas showed robust protein expression resulting from the AAV-mediated PDE6α′ expression in both rods and cones as driven by the smCBA promoter. In contrast, the WT control displays a weaker immunoreactive band as a result of the presence of PDE6α′ in cones only. INL, Inner nuclear layer; ONL, outer nuclear layer.

and Beavo, 1988; Hamilton and Hurley, 1990; Li et al., 1990). Each of the catalytic subunits of PDE6 consists of two N-terminal regulatory cGMP binding GAF (for cGMP-specific phosphodiesterases, adenylyl cyclases, and FhlA) domains (GAFa and GAFb) and a catalytic domain located in the C-terminal region. The catalytic domains are highly conserved among rod and cone PDE6 subunits and exhibit equivalent enzymatic activities (Mou and Cote, 2001; Muradov et al., 2010). Among the GAF domains, rod PDE6 GAF displays a higher affinity toward cGMP than cone PDE6 (Gillespie and Beavo, 1989). It has been suggested that the differences in GAF binding affinities toward cGMP and PDE6γ might contribute to the higher efficiency of cone PDE6 activation by transducin α-subunit (Muradov et al., 2010).

In this study, we tested whether PDE6 catalytic subunit identity contributes to the functional differences between rods and cones by expressing cone PDE6α′ in the retinal degeneration 10 (*rd10*) photoreceptor cells, which carry a mutation in the β-subunit of rod PDE6 (Chang et al., 2007). We show that cone PDE6α′ can restore *rd10* rod function by assembling with rod PDE6γ. Furthermore, it confers rods with distinct physiological properties.

Materials and Methods

Animals. *rd10* mice and wild-type (WT) C57BL/6J controls were obtained from The Jackson Laboratory. The mice of either sex were bred and maintained in the University of Florida Health Science Center Animal Care Services Facilities in a continuously dark room, except for husbandry at ~400 lux illuminance. All experiments were approved by the local Institutional Animal Care and Use Committees at the University of Florida and Washington University and conducted in accordance with the Association for Research in Vision and Ophthalmology Statement for the Use of Animals in Ophthalmic and Vision Research and National Institutes of Health regulations.

Construction and packaging of adeno-associated virus vectors. PDE6α′ cDNA was purchased from Invitrogen. The adeno-associated virus (AAV) vector containing murine PDE6α′ or PDE6β cDNA under the control of small chicken β-actin (smCBA) promoter was packaged in AAV serotype 8 (AAV8) Y733F by transfection of HEK293 cells according to previously published methods (Zolotukhin et al., 1999).

Subretinal injections. Postnatal day 14 (P14) *rd10* pups raised in the dark were brought to a normal illuminated room for injection and then returned back to dark. A total volume of 1 μl of AAV8 Y733F–smCBA–PDE6α′ vector (4.25×10^{12} vector genomes/ml) was injected subretinally into the left eyes, and the right contralateral eyes served as untreated controls. Subretinal injections were performed as described previously (Pang et al., 2006, 2008). Briefly, a 33 gauge blunt needle mounted on a 5 μl Hamilton syringe was introduced through the corneal opening made by 30 gauge needle, and injections were visualized by fluorescein-positive subretinal bleb. One percent atropine eye drops and neomycin/polymyxin B/dexamethasone ophthalmic ointment were given after injection.

Electroretinogram analyses. At 5 weeks after injection, rod- and cone-mediated electroretinograms (ERGs) were recorded separately using a UTAS Visual Diagnostic System equipped with Big Shot Ganzfeld (LKC Technologies) according to protocols described previously with minor modifications (Pang et al., 2010). Scotopic rod recordings were performed with three increasing light intensities at −1.6, −0.6, and 0.4 log cds/m^2. Ten responses were recorded and averaged at each light intensity. Photopic cone recording were taken after mice were adapted to a white background light of 30 cds/m^2 for 5 min. Recordings were performed with four flash intensities at 0.1, 0.7, 1.0, and 1.4 log cds/m^2 in the presence of 30 cds/m^2 background light. Fifty responses were recorded and averaged at each intensity. Scotopic and photopic b-wave amplitudes from untreated, treated *rd10*, and WT controls at each intensity were averaged and used to generate an SD. The differences between recordings from untreated and treated eyes were analyzed by the paired *t* test.

Morphology and immunohistochemistry. Treated *rd10* mice were killed and enucleated 2 d after ERG recordings for morphological and immunohistochemical analysis. The eyecups were fixed in a mixture of 4.0% paraformaldehyde and 0.5% glutaraldehyde for 3 h at room temperature and then paraffin embedded and sectioned at 4 μm through the optic nerve for hematoxylin and eosin (H&E) staining. Retinal sections for immunohistochemistry were prepared according to previously described methods (Deng et al., 2009, 2012). Briefly, eyes were fixed in 4% paraformaldehyde. Cornea, lens, and vitreous were removed from each eye without disturbing the retina. The remaining eyecup was rinsed with PBS and then cryoprotected by placing it in 30% sucrose in PBS for 4 h at 4°. Eyecups were then embedded in cryostat compound (Tissue TEK OCT; Sakura Finetek) and frozen at −80°C. Retinal tissue cryosections were sectioned at 12 μm thickness, rinsed in PBS, and blocked in 2% normal goat serum and 0.3% Triton X-100 in 1% BSA in PBS for 1 h at room temperature. Anti- PDE6α′ (3184P) (Kirschman et al., 2010), rhodopsin, or red/green-cone opsin (Millipore Bioscience Research Reagents) antibodies (all 1:1000 dilutions) were diluted in 0.1% Triton X-100 and 1% BSA in PBS and incubated with sections overnight at 4°. The sections were then washed three times with PBS, incubated with IgG secondary antibody tagged with Alexa Fluor-594 (Invitrogen) at 1:500 dilution and lectin peanut agglutinin (PNA) conjugated to Alexa Fluor-488 (Invitrogen) at 1:200 dilution in PBS at room temperature for 1 h, and washed with PBS. Sections were mounted with Vectashield Mounting Medium for Fluorescence (H-1000; Vector Laboratories) and coverslipped. Sections were analyzed with a Carl Zeiss CD25 microscope fitted with Axiovision release 4.6 software.

Western blot analyses. Untreated, AAV8 Y733F–smCBA–PDE6α′-treated *rd10* and WT eyes (five eyes each) were carefully dissected, and the eyecups were pooled and homogenized by sonication in a buffer containing 0.23 M sucrose, 5 mmol/L Tris-HCl, pH 7.5, and protease inhibitors (Roche Complete). After centrifugation, aliquots of the ex-

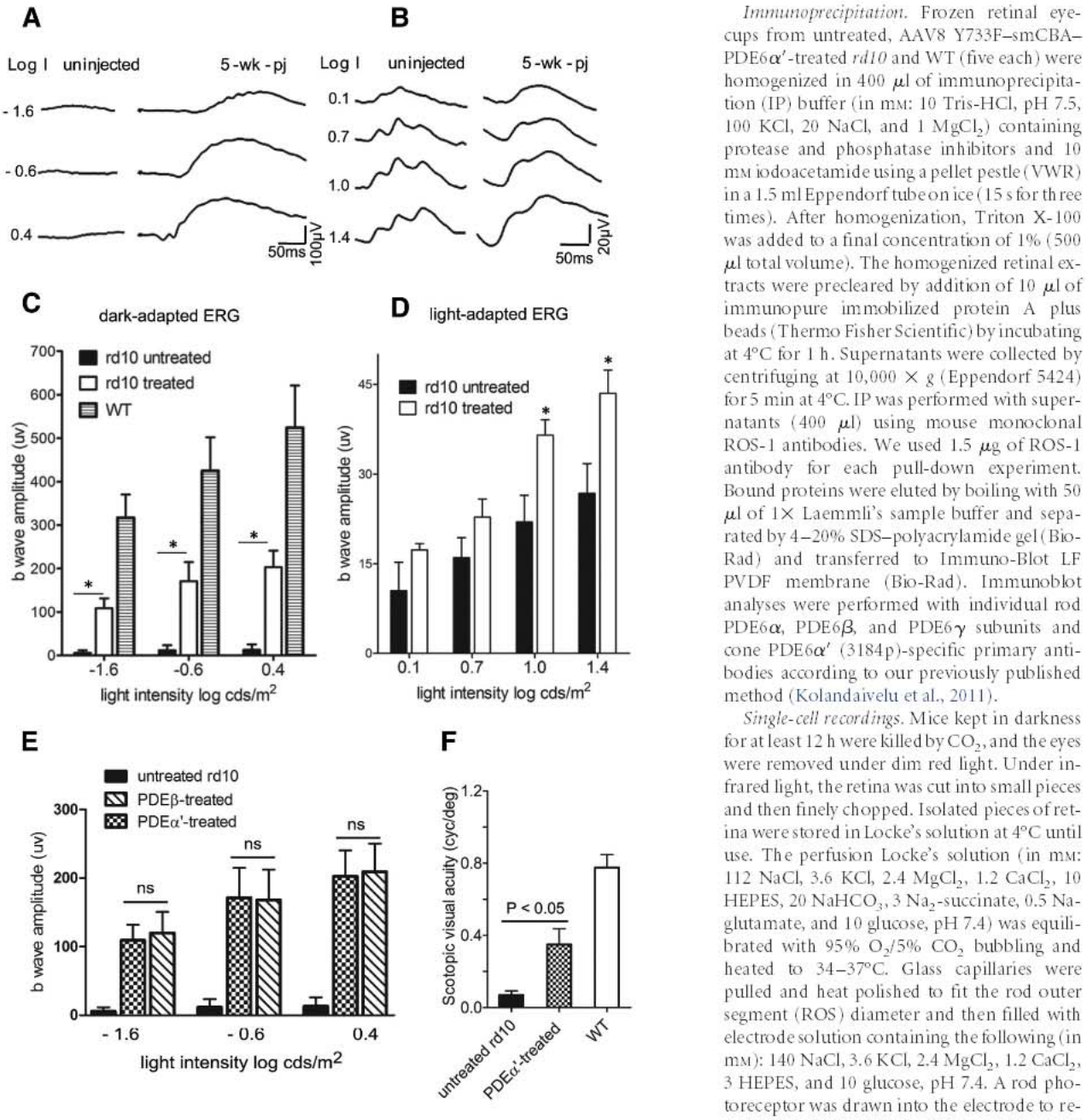

Figure 2. ERG responses, retinal morphology, immunohistochemistry, and scotopic visual acuity of *rd10* mice after AAV8 Y733F–smCBA–PDE6α′ delivery at 5 weeks after injection (5-wk-pj). ***A***, ***B***, Representative examples of dark-adapted ERG traces (***A***) and light-adapted ERG traces (***B***) from an *rd10* mouse at 5 weeks after injection. ***C***, Dark-adapted ERG was partially restored in injected *rd10* eyes. Statistical analysis demonstrated a significant difference between uninjected and fellow vector-treated eyes for dark-adapted b-waves at −1.6, −0.6, and 0.4 log cds/m^2 (*$p < 0.01$). ***D***, Light-adapted ERG responses were improved in treated *rd10* eyes compared with their contralateral controls as a result of rod function rescue and rod cell survival (*$p < 0.02$). Error bars are mean ± SD. ***E***, Comparison of ERG responses between PDE6β-treated and PDE6α′-treated *rd10* eyes 5 weeks after injection. There were no significant differences in dark-adapted b-wave amplitudes at three light intensities tested between PDE6β-treated and PDE6α′-treated *rd10* eyes (all $p > 0.1$). Bar graph representing the mean ± SEM. b-Wave amplitudes at indicated flash intensities were compared by repeated-measures ANOVA, with the Bonferroni's *post hoc* test for ANOVA ($p < 0.1$) used to compare means at individual flash intensities. ***F***, Restoration of scotopic visual acuity in PDE6α′-treated *rd10* mice 5 weeks after injection. Data were derived from mouse optomotor responses to rotating gratings under background monitor luminance of −4.45 log cd/m^2. Bar graphs are mean ± SEM.

tracts containing equal amounts of protein (50 μg) were analyzed by electrophoresis on 10% polyacrylamide–SDS gels, transferred, and probed with a PDE6α′ antibody (Kolandaivelu et al., 2011). An antibody against α-tubulin (rabbit polyclonal ab4074; Abcam) was used as an internal control. Visualization of specific bands was performed using the Odyssey Infrared Fluorescence Imaging System (Odyssey; Li-Cor).

Immunoprecipitation. Frozen retinal eyecups from untreated, AAV8 Y733F–smCBA–PDE6α′-treated *rd10* and WT (five each) were homogenized in 400 μl of immunoprecipitation (IP) buffer (in mM: 10 Tris-HCl, pH 7.5, 100 KCl, 20 NaCl, and 1 $MgCl_2$) containing protease and phosphatase inhibitors and 10 mM iodoacetamide using a pellet pestle (VWR) in a 1.5 ml Eppendorf tube on ice (15 s for three times). After homogenization, Triton X-100 was added to a final concentration of 1% (500 μl total volume). The homogenized retinal extracts were precleared by addition of 10 μl of immunopure immobilized protein A plus beads (Thermo Fisher Scientific) by incubating at 4°C for 1 h. Supernatants were collected by centrifuging at 10,000 × *g* (Eppendorf 5424) for 5 min at 4°C. IP was performed with supernatants (400 μl) using mouse monoclonal ROS-1 antibodies. We used 1.5 μg of ROS-1 antibody for each pull-down experiment. Bound proteins were eluted by boiling with 50 μl of 1× Laemmli's sample buffer and separated by 4–20% SDS–polyacrylamide gel (Bio-Rad) and transferred to Immuno-Blot LF PVDF membrane (Bio-Rad). Immunoblot analyses were performed with individual rod PDE6α, PDE6β, and PDE6γ subunits and cone PDE6α′ (3184p)-specific primary antibodies according to our previously published method (Kolandaivelu et al., 2011).

Single-cell recordings. Mice kept in darkness for at least 12 h were killed by CO_2, and the eyes were removed under dim red light. Under infrared light, the retina was cut into small pieces and then finely chopped. Isolated pieces of retina were stored in Locke's solution at 4°C until use. The perfusion Locke's solution (in mM: 112 NaCl, 3.6 KCl, 2.4 $MgCl_2$, 1.2 $CaCl_2$, 10 HEPES, 20 $NaHCO_3$, 3 Na_2-succinate, 0.5 Na-glutamate, and 10 glucose, pH 7.4) was equilibrated with 95% O_2/5% CO_2 bubbling and heated to 34–37°C. Glass capillaries were pulled and heat polished to fit the rod outer segment (ROS) diameter and then filled with electrode solution containing the following (in mM): 140 NaCl, 3.6 KCl, 2.4 $MgCl_2$, 1.2 $CaCl_2$, 3 HEPES, and 10 glucose, pH 7.4. A rod photoreceptor was drawn into the electrode to record the inward current of the outer segment (OS). The dark current was amplified by a current-to-voltage converter (Axopatch 200B; Molecular Devices), low-pass filtered by an eight-pole Bessel filter with a cutoff frequency of 30 Hz (Krohn-Hite), digitized at 1 kHz, and recorded with pClamp 8.2 software (Molecular Devices). Ten-millisecond flashes were delivered from a calibrated light source via computer-controlled shutters. Light intensity and wavelength were changed with neutral density and interference (λ_{max} = 500 nm) filters (Edmund Optics). Intensity–response data were fit by the Hill equation: $\frac{R}{R_{max}} = \frac{I^n}{I^n + I_o^n}$, where R is the transient-peak amplitude of response, R_{max} is maximal response amplitude, I is flash intensity, and I_o is flash intensity to generate half-maximal response.

Visual acuity test. Scotopic visual acuity of 2-month-old mice was determined using a two-alternative forced-choice protocol (Umino et al.,

2008). The Optomotry system (Cerebral Mechanics) consisted of a square array of four computer monitors with a pedestal in the center where the mouse was placed. An infrared-sensitive television camera and a round array of six infrared light-emitting diodes mounted above the animal were used to observe the mouse but not the monitors. Using a staircase paradigm, rotating sine-wave vertical gratings were applied on the monitors where they formed a virtual cylinder around the animal (Prusky et al., 2004). The mice responded to the stimuli by reflexively rotating their head in either clockwise or counterclockwise direction. Optomotor responses were measured under monitor background illumination of −4.45 log cd/m^2, which was set by neutral density film filters.

Visual acuity was defined as the threshold for spatial frequency (F_s) of gratings with 100% contrast and measured at the speed (S_p) of 6.0°/s. F_s was gradually altered by the computer protocol until its combined threshold for both stimuli directions was determined. Temporal frequency (F_t) was automatically adjusted by the computer software, based on the following equation: $F_t = S_p \times F_s$ (Umino et al., 2008). Data were analyzed using independent two-tailed Student's *t* test, with an accepted significance level of $p < 0.05$.

Results

Expression of cone PDE6α′ in rd10 mouse retinas

An AAV8 Y733F capsid-tyrosine mutant vector containing the mouse *PDE6α′* cDNA driven by a ubiquitous smCBA promoter was delivered subretinally to one eye of *rd10* mice at P14, whereas the contralateral eyes remained uninjected and served as controls. PDE6α′ expression in treated retinas was analyzed by immunostaining (Fig. 1*A*) and Western blot analysis (Fig. 1*B*) at 5 weeks after injection. PDE6α′ expression was found in both rods and cones of treated *rd10* mice after immunostaining with a cone-specific PDE6α′ antibody, whereas it was found exclusively in the cones of WT control mouse retinas based on colocalization with a cone OS sheath-specific PNA marker. Photoreceptor cells in untreated retinas were significantly degenerated at this age, and only a weak spotty staining was detected for residual cones (Fig. 1*A*). Low levels of expression were also observed in the inner retina most likely as a result of nonspecificity of the PDE6α′ antibody because similar labeling was observed in untreated and treated *rd10*, as well as in the WT sections (Fig. 1*A*). Western blot analysis using the same antibody (Fig. 1*B*) detected abundant PDE6α′ expression in injected *rd10* retinas compared with WT controls in which PDE6α′ was expressed predominantly in cones. This result provides evidence that PDE6α′ is robustly expressed in *rd10* rods after AAV8 treatment because rods comprise the majority (97%) of photoreceptor cells in the mouse retina. PDE6α′ expression was reduced to almost undetectable levels in retina from uninjected *rd10* animals (Fig. 1*B*), presumably because of the degeneration of cones caused by the loss of PDE6β-deficient rods.

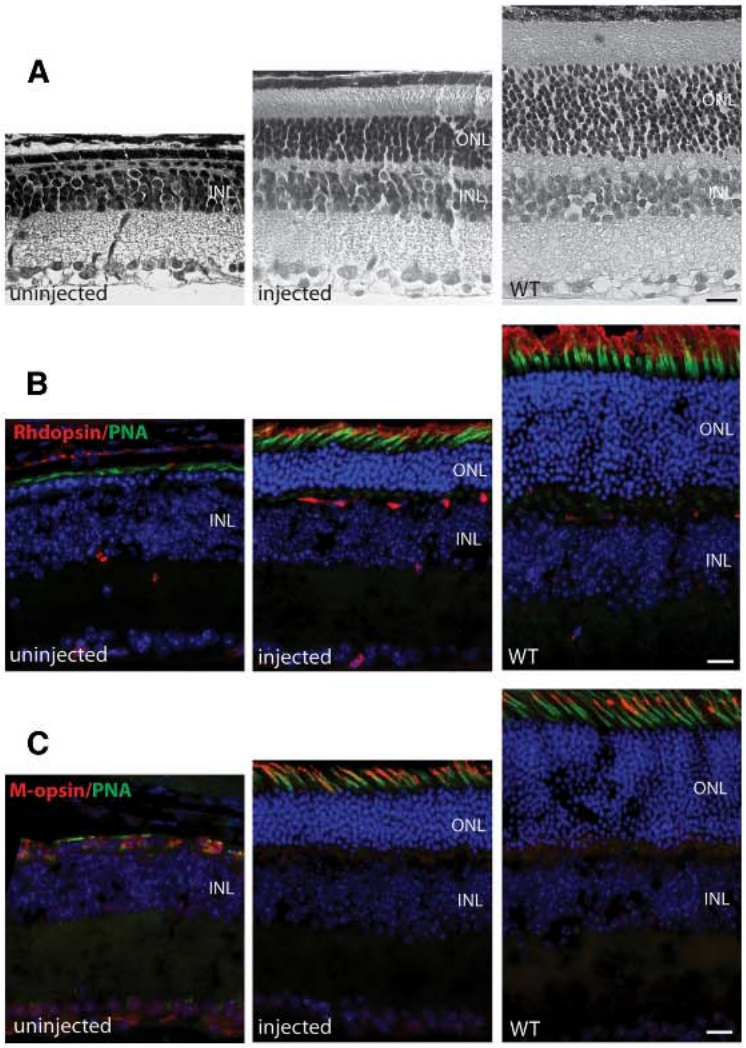

Figure 3. ***A***, Light micrographs of uninjected, injected *rd10*, and WT mouse retinas. ***B***, Immunostaining of uninjected, injected *rd10*, and WT retinas with rhodopsin antibody (red). ***C***, Immunostaining of uninjected, injected *rd10*, and WT retinas with red/green cone opsin antibody (red). Green, Cone OS sheath-specific PNA. Scale bar, 20 μm. INL, Inner nuclear layer; ONL, outer nuclear layer.

Functional and structural retinal preservation in PDE6α′-treated rd10 eyes

To determine whether exogenously expressed cone PDE6α′ can rescue rod function in *rd10* mice, full-field scotopic and photopic ERG responses were recorded from uninjected *rd10* mice, injected *rd10* mice 5 weeks after injection, and age-matched WT controls. Rod-mediated ERG responses were undetectable in *rd10* mice at this age (7 weeks old), whereas vector delivery of PDE6α′ to *rd10* rods led to significant restoration of rod-driven ERG responses (Fig. 2*A*,*C*). The average rod-mediated b-wave amplitude at a flash intensity of −1.6 log cds/m^2 in treated eyes was 109 ± 39 μV (mean ± SD), whereas it was undetectable in contralateral untreated eyes ($n = 3$, $p < 0.01$). The treated eye rod ERG b-wave amplitude was ~35% of the WT level. Cone-mediated ERG amplitudes in injected eyes also showed some improvement compared with uninjected controls (Fig. 2*B*,*D*), presumably as a result of better preservation of the cones after restoration of rod function and rod survival (Fig. 3*C*). The average cone b-wave amplitude was 44 ± 8 μV (mean ± SD) in injected eyes versus 27 ± 10 μV in contralateral untreated eyes at 1.4 log cds/m^2 ($n = 3$, $p < 0.02$). We also recorded ERG responses

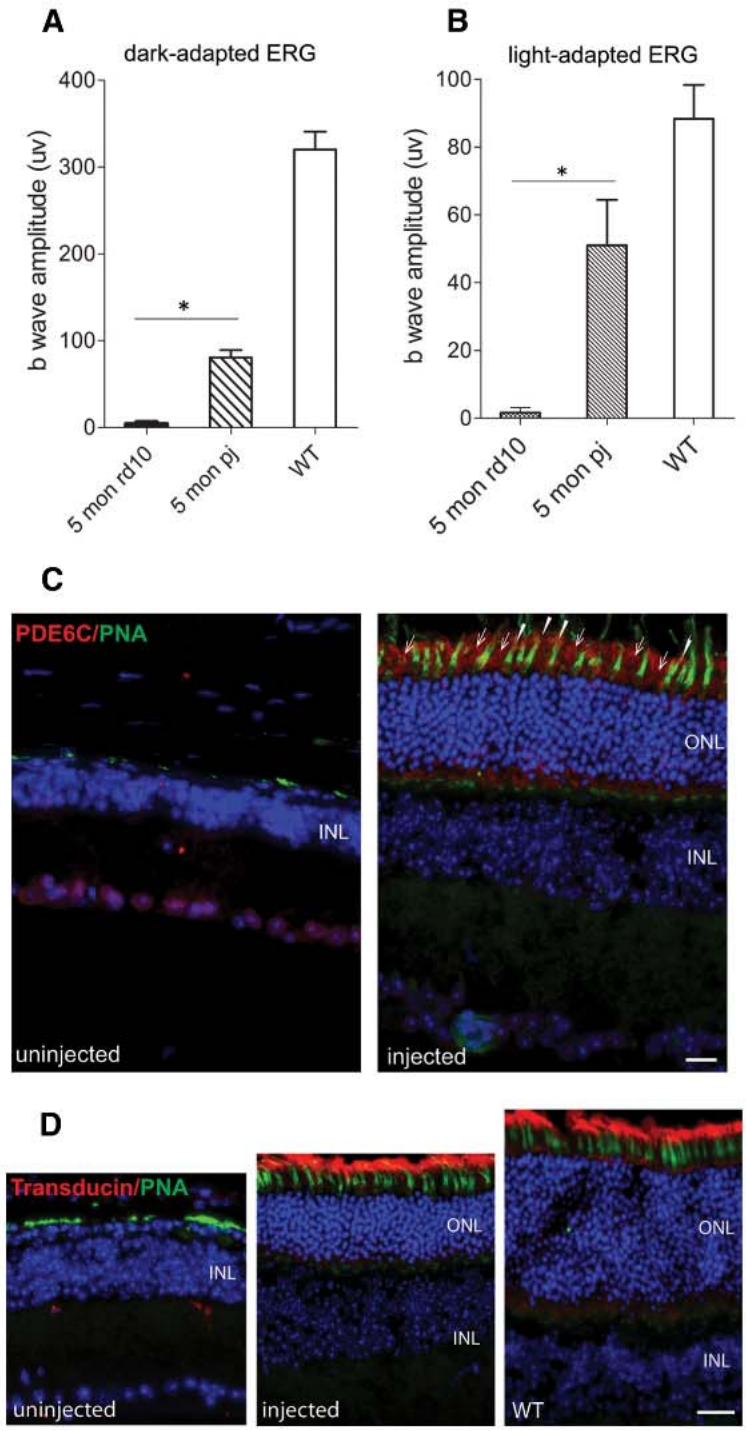

Figure 4. ERG rescue and immunohistochemistry of *rd10* mice 5 months after injection (5 mon pj). ***A***, Dark-adapted ERG from uninjected, contralateral injected *rd10*, and WT control eyes at light intensity of 0.4 log cds/m^2 (*$p < 0.005$). ***B***, Light-adapted ERG from the same mice at light intensity of 1.0 log cds/m^2 (*$p < 0.03$). Error bars are mean ± SD. ***C***, PDE6α′ expression 5 months after delivering AAV8 Y733F–smCBA–PDE6α′ in *rd10* retinas. Immunofluorescence of PDE6α′ (labeled as red) can be detected in both rods (arrows) and cones (arrow heads) in injected *rd10* retinas. Only spotty staining was found in untreated eye as a result of significant retina degeneration. Cones were labeled by PNA (green). ***D***, Immunostaining of uninjected, injected *rd10*, and WT retinas with transducin antibody (red). Green, Cone OS sheath-specific PNA. Scale bar, 20 μm. INL, Inner nuclear layer; ONL, outer nuclear layer.

from some *rd10* mice injected with vector expressing PDE6β and observed no significant differences between PDE6β and PDE6α′ treatments (Fig. 1*E*), suggesting that therapy in the *rd10* mouse was equivalent whether we used the heterologous rod subunit or the homologous cone subunit. Finally, the scotopic visual acuity of PDE6α′-treated *rd10* mice improved significantly (0.349 ± 0.088, $n = 8$) over that of untreated controls (0.069 ± 0.024, $n = 5$) (Fig. 2*F*), although rod visual performance still remained subpar compared with WT mice (0.776 ± 0.072).

Three *rd10* mice exhibiting significant ERG rescue were killed 2 d after the recordings, and retinal morphology was analyzed by H&E staining (Fig. 3*A*). Only one layer of photoreceptor nuclei remained in the outer nuclear layer of untreated *rd10* retinas with no evident outer or inner segments. In contrast, retinal structure was partially preserved in injected eyes, with five to seven layers of nuclei remaining compared with 12 layers in WT controls. Additionally, treated retinas retained ~20–50% of the normal OS length. Uninjected, injected, and WT retinal sections were also stained with rhodopsin antibody (Fig. 3*B*) and cone opsin-specific (Fig. 3*C*) antibody to further confirm the morphological rescue. Expression of both rhodopsin and cone opsin was evident and much more abundant in treated *rd10* eyes compared with their spotty staining observed in uninjected controls.

We also recorded ERG responses from *rd10* mice at 5 months after treatment (Fig. 4 *A*,*B*). The average rod-driven ERG b-wave amplitude (Fig. 4*A*) at a flash intensity of −1.6 log cds/m^2 in treated eyes was 81 ± 15 μV (mean ± SD), and it was significantly higher than the undetectable ERGs in uninjected eyes ($n = 3$, $p < 0.005$). The cone-mediated ERG responses (Fig. 4*B*) were also undetectable in untreated eyes at this age, whereas the average b-wave amplitude in treated eyes at 1.0 log cds/m^2 was 51 ± 13 μV (mean ± SD) ($n = 3$, $p < 0.03$). PDE6α′ expression was still evident in both rods and cones in treated eyes at 5 months after injection (Fig. 4*C*). Transducin was strongly expressed in the treated eyes as determined by immunostaining, whereas it was undetectable in untreated eyes at 5 months after injection (Fig. 4*D*). Thus, PDE6α′-mediated rescue of *rd10* rod structure and function persisted even months after the AAV injection.

Cone PDE6α′ binds to rod PDE6γ to restore rod function

Restoration of the light-dependent rod response in *rd10* animals suggested that PDE6α′ expressed by AAV is capable of forming a functional complex with rod PDE6γ. Before testing this idea, we investigated the levels of various subunits of rod PDE6 holoenzyme. Uninjected *rd10* animals with advanced stage of rod degeneration lacked all three subunits of rod PDE6 (Fig. 5*A*). Despite preservation of five to eight layers of photoreceptor cells in injected animals, we observed destabilization of both rod

PDE6 catalytic subunits (Fig. 5*A*). Compared with age-matched WT controls, minor amounts of PDE6α or PDE6β were expressed in total retinal extracts from injected animals. In contrast, there was a dramatic upregulation in PDE6α′ expression in these retinas. Although lower than in WT controls, we observed robust expression of rod PDE6γ in treated animals likely as a result of complex formation with the virally introduced PDE6α′. To directly test whether the formation of a complex between cone PDE6α′ and rod PDE6γ existed, we performed IP with a monoclonal antibody, ROS-1, that exclusively recognizes assembled and functional PDE6 complex from both rods and cones (Kolandaivelu et al., 2009, 2011). As expected, we observed assembled rod and cone PDE6 subunits in ROS-1 pull-downs from WT controls (Fig. 5*B*). Assembled PDE6α′ was also observed from surviving cones in uninjected animals. In treated *rd10* animals, we detected a complex of PDE6α′ and PDE6γ indicating that the restoration of light sensitivity in *rd10* rods is attributable to the function of cone PDE6α′ assembled with rod PDE6γ (Fig. 5*B*).

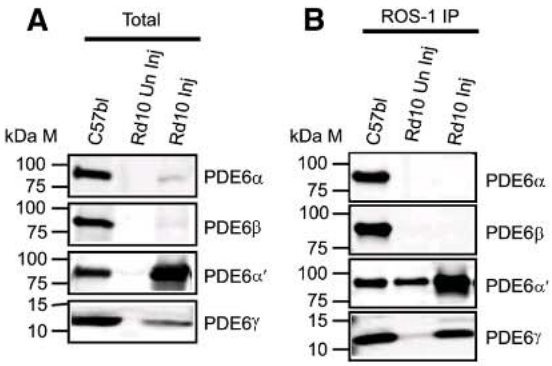

Figure 5. Cone PDE6α′ subunit expressed in rods associates with rod PDE6γ inhibitory subunit. ***A***, Immunoblot analysis with indicated antibodies show the total levels of PDE6 subunits in retinal extracts from WT control, *rd10* uninjected (Rd10 Un Inj), and *rd10*-injected (Rd10 Inj) animals. ***B***, IP of assembled PDE6 subunits with ROS-1 antibody from retinal extracts of WT control, uninjected *rd10*, and injected *rd10* animals. After ROS-1 IP, immunoblots were probed with indicated antibodies. Compared with total extracts (***A***), IP samples (***B***) were 10 times more concentrated.

Single-cell recordings from injected rd10 rods

To gain additional insight into the light responses generated by rods expressing cone PDE6α′, we performed single-cell recordings from injected *rd10* rods and WT controls. For comparison, we also obtained responses from *rd10* rods treated with vector expressing rod PDE6β. Although all retinas of PDE6α′- and PDE6β-treated *rd10* mice were still subject to some level of degeneration, we were able to find areas with healthy ROS in portions of the retina in which AAV vectors seemed to have been successfully delivered. We obtained photoresponses from 14 PDE6α′-treated rods (from two animals) and 22 PDE6β-treated rods (from three animals). No significant differences were found between the photoresponses of WT and PDE6β-treated *rd10* rods (compare with Fig. 6*A*,*C*, Table 1), indicating that the exogenous expression of PDE6β by AAV infection into rods of *rd10* mice successfully rescued rod physiological functions. The dark currents, measured from saturated photoresponses, were comparable among WT, PDE6β-treated, and PDE6α′-treated rods (Table 1). Thus, PDE6α′ ectopically expressed in rod photoreceptors could form a functional complex with rod PDE6γ and maintain normal spontaneous activity and dark cGMP levels. However, we also observed several unusual features in the responses of PDE6α′-treated rods. First, PDE6α′-treated rods had higher sensitivity and produced larger single-photon responses than WT rods (Fig. 7*A*, Table 1). Consistent with this result, intensity–response relationships of dark-adapted rods showed that the flash intensity required for half-saturating response of the PDE6α′-treated rods was approximately twofold lower than that of WT rods (Fig. 6*D*, inset, Table 1). Second, the time-to-peak and integration time of dim-flash responses were substantially prolonged in PDE6α′-treated *rd10* rods (Fig. 7*A*, Table 1). The rising phase of dim-flash response was similar among WT, PDE6β-treated, and PDE6α′-treated *rd10* rods (Fig. 7*A*), which indicates that light-induced cGMP hydrolysis activated by PDE occurred at comparable rates. However, the response recovery phase was substantially delayed in PDE6α′-treated rods, indicating that the deactivation of cone PDE6α′ was less effective. This slower than normal response shutoff could potentially explain the increased sensitivity and single-photon response amplitude in PDE6α′-treated *rd10* rods. Third, unlike in WT and PDE6β-treated *rd10* rods, the response kinetics in PDE6α′-treated rods accelerated substantially with increasing flash strength (Fig. 6*B*), and the resulting intensity–response curves appeared shallower than these of WT and control PDE6β-treated *rd10* rods. Both of

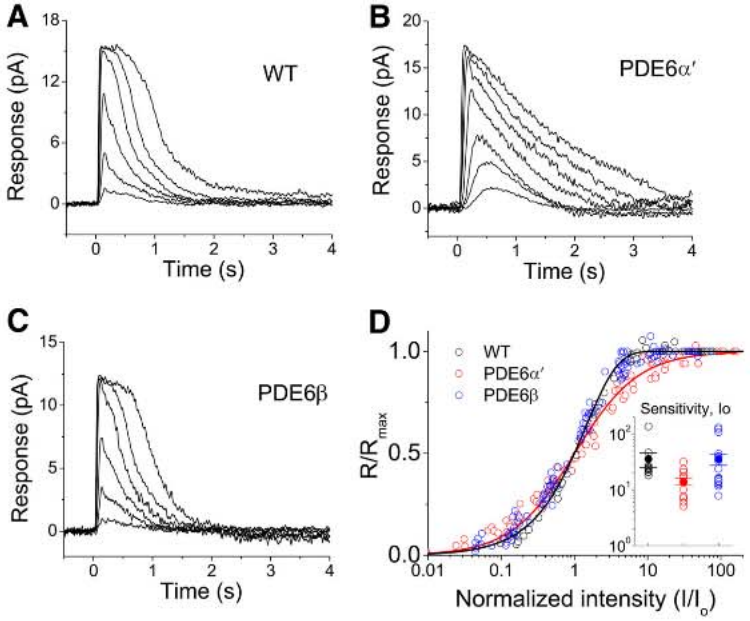

Figure 6. Typical flash response families from single-cell recordings obtained from WT (***A***), PDE6α′-treated (***B***), and PDE6β-treated (***C***) *rd10* rods. Flashes of intensities increasing in 0.5 log unit steps were delivered at time 0 with duration of 10 ms. Dimmest flash intensities were 3.6, 0.61, and 1.8 photons/μm^2 in the WT, PDE6α′-treated, and PDE6β-treated rods, respectively. ***D***, Fractional response (R/R_{max}) of individual rods as a function of flash intensity (I) normalized for half-saturating flash intensity (I_o). Data from WT rods (black circles, $n = 10$), PDE6β-treated *rd10* rods (blue circles, $n = 22$), and PDE6α′-treated *rd10* rods (red circles, $n = 14$) are well fit by saturating-exponential function and by Hill equation with $n = 0.95$, respectively. Inset, Cumulative data of sensitivity (I_o) from individual rods (open circles). Mean values are represented as filled circles. Error bars are mean ± SEM.

Table 1. Rod response parameters of single-cell recordings

	WT ($n = 10$)	PDE6α′ ($n = 14$)	PDE6β ($n = 22$)
Dark current (pA)	16.0 ± 1.0	14.8 ± 1.1	13.5 ± 0.8
Sensitivity, I_o (photons μm^{-2})	35.7 ± 10.4	14.1 ± 2.1	35.2 ± 7.7
Time-to-peak (ms)	169 ± 9	487 ± 21*	178 ± 7
Integration time (ms)	448 ± 34	790 ± 35*	495 ± 29
Single-photon response (pA)	0.71 ± 0.08	1.55 ± 0.22*	0.76 ± 0.09

Mean ± SEM integration time was calculated by dividing the area of dim-flash response by its amplitude. Amplitude of single-photon response was estimated from variance/mean ratio of dim-flash responses evoked by consecutive identical stimuli. One-way ANOVA with the *post hoc* Tukey's HSD test determined significant differences (*$p < 0.05$ vs WT and PDE6β). No significant difference was found between WT and PDE6β parameters.

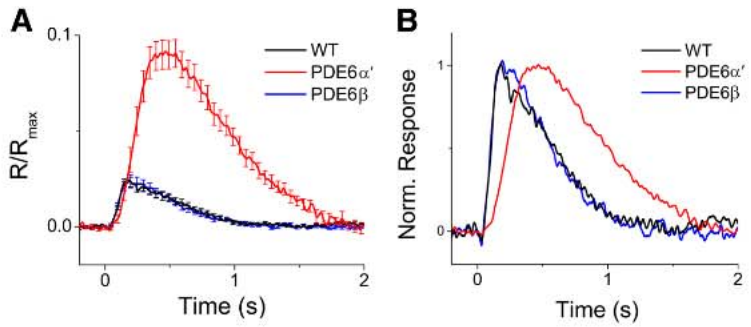

Figure 7. ***A***, Single-photon responses from WT (black), PDE6α′-treated (red), and PDE6β-treated (blue) *rd10* rods. Single-photon responses were obtained by dividing each dim-flash response (<0.2 R_{max}) by the estimated number of activated rhodopsins per rod, with the collecting area assumed to be 0.5 μm^2. The traces are averaged from 10 WT, 14 PDE6α′-treated, and 22 PDE6β-treated individual cells. Error bars represent SEM. ***B***, Comparison of dim-flash responses scaled at peak amplitude.

these response features suggest a possible light-dependent feedback modulation directly on cone PDE6α′.

Discussion

In this study, we expressed cone PDE6α′ subunit exogenously in the retinas of *rd10* mice to investigate its biochemical and light signaling properties in a rod cell environment. Our results demonstrate that cone PDE6α′ can functionally substitute for rod PDE6αβ to mediate light signaling in rods, as shown by full-field ERG analysis, behavioral experiments, and single-cell recordings. Rod PDE6 catalytic subunits are destabilized in PDE6α′-injected retinas despite the functional and morphological rescue of rods, and restoration of rod light sensitivity is mediated by assembly of cone PDE6α′ with rod PDE6γ. Rods with cone PDE6α′ are approximately two times more sensitive to light than WT cells, and this difference is likely the result of the slower shutoff of their light responses. The slower rate of deactivation indicates that inhibition by rod PDE6γ or the hydrolysis of Tα*–GTP on PDE6α′–transducin α complex by regulator of G-protein signaling-9 (RGS9) is less efficient than normal.

We demonstrated previously that AAV-mediated subretinal delivery of rod PDE6β transgene confers long-term rescue of visual function and morphological preservation of the *rd10* retinas (Pang et al., 2011). In the present study, AAV8 Y733F cone PDE6α′-treated *rd10* retinas showed comparable levels of rescue in gross morphology, amplitudes of rod-driven full-field ERG signals, and the maximal amplitude of single-photon responses, clearly demonstrating that cone PDE6α′ can couple effectively to the rod visual signaling pathway in response to light. Our work complements the previous finding of the ability of rod PDE6 to substitute for cone PDE6 to mediate visual signaling in $Nrl^{-/-}$*cpfl1* mouse model (Kolandaivelu et al., 2011). Although the PDE6α′ transgene was driven by an smCBA ubiquitous promoter, we detected most PDE6α′ in photoreceptor cells in which it is normally expressed. We observed similar phenomenon of endogenous cell-specific expression in the cases of RPE65 (Pang et al., 2006), transducin (Deng et al., 2009), and PDE6β (Pang et al., 2011) proteins when using the ubiquitous CBA promoter. The significant scatter in the sensitivity of the AAV-treated rods (Fig. 6*D*, inset) most likely reflects the variability of AAV-mediated PDE6 expression.

We also showed that vector-expressed cone PDE6α′ localized properly in ROSs. It has been suggested that binding of PDE6 to OS membranes is essential for rapid activation by transducin (Liebman et al., 1987). Cone PDE6α′ ectopically expressed in rods of *Xenopus laevis* was shown to colocalize with endogenous PDE6 on disc rim regions in RODs (Muradov et al., 2009). The similar rising phases of dim-flash responses between PDE6α′-treated *rd10* and WT rods as shown with single-cell recordings suggest that the activation rate of the catalytic cone PDE6 subunit in the rod environment is comparable with that of rod PDE6 and that exogenously expressed cone PDE6α′ is appropriately localized to ROS disk membranes.

We further show that the restoration of light sensitivity in *rd10* rods is attributable to the assembly of cone PDE6α′ with rod PDE6γ. Robust expression of PDE6γ was observed in injected retinas, most likely as a result of complex formation with the virus-introduced PDE6α′. The presence of cone PDE6α′ or restoration of rod cells did not help in preserving rod PDEα, which was degraded without its PDEβ partner. It appears that, regardless of cell type, cone PDE6α′ forms homodimers to be functional *in vivo*. The same holds true for rod PDE6 in the sense that PDE6α and PDE6β are obligated to function as heterodimers (Kolandaivelu et al., 2011). Apparently, the state of association is determined by the properties of the subunits rather than the photoreceptor cell type. All families of vertebrate cyclic nucleotide phosphodiesterases function as homodimers, and, although the reason behind the heterodimerization of rod PDE6 is not known, it presumably exists as a mechanism to control the amount of functional PDE6 enzyme present in rods (Kolandaivelu et al., 2011).

The equivalent rate of activation between WT rods and *rd10* rods expressing cone PDE6α′ or PDE6β suggests that activated Tα*–GTP can effectively release the inhibitory constrain of rod PDE6γ from cone PDE6α′ catalytic domain. However, the slower shutoff of PDE6α′-treated rods indicates that deactivation of cone PDE6α′ by inhibitory rod PDE6γ or the hydrolysis of α-subunit-bound GTP on PDE6α′–transducin complex is less efficient. The GAFa domains also bind to the inhibitory γ subunits and play a role in the dimerization of the PDE6 catalytic subunits (Muradov et al., 2004). The strength of interaction between PDE6γ and GAF domains is modulated by cGMP binding to GAF domain. cGMP binding induces an allosterical GAF conformational change and enhances PDE6γ binding affinity, and, in a reciprocal manner, binding of γ-subunit to PDE6 catalytic dimer increases the binding affinity of cGMP to the GAF domains (Yamazaki et al., 1982; Cote et al., 1994). Accordingly, dissociation of either one weakens the binding of the other. Based on a structural study of PDE6γ (Barren et al., 2009), it has been suggested that the interaction between Tα*–GTP and PDE6γ induces a hinge-like movement of the last 10 residues away from

the enzyme active site without the Tα*–GTP/PDE6γ complex completely disassociating from the PDE6 holoenzyme. The inactivation of Tα*–GTP by its intrinsic GTPase activity is the rate-limiting step to restore the photoresponse to a dark-adapted state and its regulator RGS9-1 associates with PDE6γ to accelerate the GTPase activity of Tα*–GTP (Arshavsky and Burns, 2012). The multiple interactions of PDE6γ with PDE6αβ, Tα*–GTP, and RGS9-1 complex are likely to occur in a precisely controlled temporal sequence that coordinates the activation and deactivation of PDE6 (Zhang et al., 2012). The major sequence difference between cone and rod PDE6 resides in the GAF domains, with cone PDE6 displaying a lower affinity toward cGMP. The relative affinity of rod PDE6γ binding to Tα*–GTP versus the PDE6 catalytic subunits may be defined by the state of cGMP occupancy on the GAF domains of PDE6α′. Likewise, the affinity of rod PDE6γ for vector-expressed cone PDE6α′ may be lower than that for the rod PDE6αβ. These differences may contribute to the slower inactivation of the cone PDE6α′ expressed in rods. It would be interesting to study the effects of replacing rod PDE6γ with cone PDE6γ′ or the entire rod PDE holoenzyme with cone PDE6, because PDE6γ critically regulates phototransduction through on and off interactions with PDE6αβ, Tα*–GTP, and RGS9-1. Overall, it is difficult from our results to gain a clear view of the role of PDE in the differences in sensitivity or kinetics between rods and cones. Interestingly, although rods and cones share the same GAP complex, cones express RGS9 at higher levels (Zhang et al., 2003). This observation, together with the slow inactivation of cone PDE6α′ in rods observed by us indicate that, perhaps, the timely Tα*–GTP/PDE complex inactivation in cones requires higher GAP activity than in rods.

Finally, our single-cell recordings from cone PDE6α′-treated *rd10* rods demonstrated an unusual response acceleration with increasing flash strength. This, together with a shallower intensity–response curve for these rods indicates a potential acceleration of cone PDE inactivation with increased phototransduction activation. A direct modulation of PDE activity was recently suggested as an additional adaptation mechanism in mouse rods (Chen et al., 2012), although it has not been directly demonstrated. Notably, however, we did not observe substantial response acceleration in WT or PDE6β-treated *rd10* rods, suggesting that this is a cone PDE-specific phenomenon. Such a negative feedback modulation of cone PDE6 is an exciting novel concept and represents a potential mechanism for extending the functional range of cones. Future studies should help elucidate the mechanism(s) that regulates cone PDE6 activity and how this phenomenon affects cone light adaptation.

References

Arshavsky VY, Burns ME (2012) Photoreceptor signaling: supporting vision across a wide range of light intensities. J Biol Chem 287:1620–1626. CrossRef Medline

Barren B, Gakhar L, Muradov H, Boyd KK, Ramaswamy S, Artemyev NO (2009) Structural basis of phosphodiesterase 6 inhibition by the C-terminal region of the gamma-subunit. EMBO J 28:3613–3622. CrossRef Medline

Chang B, Hawes NL, Pardue MT, German AM, Hurd RE, Davisson MT, Nusinowitz S, Rengarajan K, Boyd AP, Sidney SS, Phillips MJ, Stewart RE, Chaudhury R, Nickerson JM, Heckenlively JR, Boatright JH (2007) Two mouse retinal degenerations caused by missense mutations in the beta-subunit of rod cGMP phosphodiesterase gene. Vision Res 47:624–633. CrossRef Medline

Chen CK, Woodruff ML, Chen FS, Shim H, Cilluffo MC, Fain GL (2010) Replacing the rod with the cone transducin subunit decreases sensitivity and accelerates response decay. J Physiol 588:3231–3241. CrossRef Medline

Chen CK, Woodruff ML, Chen FS, Chen Y, Cilluffo MC, Tranchina D, Fain GL (2012) Modulation of mouse rod response decay by rhodopsin kinase and recoverin. J Neurosci 32:15998–16006. CrossRef Medline

Cote RH, Bownds MD, Arshavsky VY (1994) cGMP binding sites on photoreceptor phosphodiesterase: role in feedback regulation of visual transduction. Proc Natl Acad Sci U S A 91:4845–4849. CrossRef Medline

Deng WT, Sakurai K, Liu J, Dinculescu A, Li J, Pang J, Min SH, Chiodo VA, Boye SL, Chang B, Kefalov VJ, Hauswirth WW (2009) Functional interchangeability of rod and cone transducin alpha-subunits. Proc Natl Acad Sci U S A 106:17681–17686. CrossRef Medline

Deng WT, Dinculescu A, Li Q, Boye SL, Li J, Gorbatyuk MS, Pang J, Chiodo VA, Matthes MT, Yasumura D, Liu L, Alkuraya FS, Zhang K, Vollrath D, LaVail MM, Hauswirth WW (2012) Tyrosine-mutant AAV8 delivery of human MERTK provides long-term retinal preservation in RCS rats. Invest Ophthalmol Vis Sci 53:1895–1904. CrossRef Medline

Fu Y, Yau KW (2007) Phototransduction in mouse rods and cones. Pflugers Arch 454:805–819. CrossRef Medline

Fu Y, Kefalov V, Luo DG, Xue T, Yau KW (2008) Quantal noise from human red cone pigment. Nat Neurosci 11:565–571. CrossRef Medline

Gillespie PG, Beavo JA (1988) Characterization of a bovine cone photoreceptor phosphodiesterase purified by cyclic GMP-sepharose chromatography. J Biol Chem 263:8133–8141. Medline

Gillespie PG, Beavo JA (1989) cGMP is tightly bound to bovine retinal rod phosphodiesterase. Proc Natl Acad Sci U S A 86:4311–4315. CrossRef Medline

Hamilton SE, Hurley JB (1990) A phosphodiesterase inhibitor specific to a subset of bovine retinal cones. J Biol Chem 265:11259–11264. Medline

Kefalov V, Fu Y, Marsh-Armstrong N, Yau KW (2003) Role of visual pigment properties in rod and cone phototransduction. Nature 425:526–531. CrossRef Medline

Kefalov VJ, Estevez ME, Kono M, Goletz PW, Crouch RK, Cornwall MC, Yau KW (2005) Breaking the covalent bond—a pigment property that contributes to desensitization in cones. Neuron 46:879–890. CrossRef Medline

Kirschman LT, Kolandaivelu S, Frederick JM, Dang L, Goldberg AF, Baehr W, Ramamurthy V (2010) The Leber congenital amaurosis protein, AIPL1, is needed for the viability and functioning of cone photoreceptor cells. Hum Mol Genet 19:1076–1087. CrossRef Medline

Kolandaivelu S, Huang J, Hurley JB, Ramamurthy V (2009) AIPL1, a protein associated with childhood blindness, interacts with alpha-subunit of rod phosphodiesterase (PDE6) and is essential for its proper assembly. J Biol Chem 284:30853–30861. CrossRef Medline

Kolandaivelu S, Chang B, Ramamurthy V (2011) Rod phosphodiesterase-6 (PDE6) catalytic subunits restore cone function in a mouse model lacking cone PDE6 catalytic subunit. J Biol Chem 286:33252–33259. CrossRef Medline

Li TS, Volpp K, Applebury ML (1990) Bovine cone photoreceptor cGMP phosphodiesterase structure deduced from a cDNA clone. Proc Natl Acad Sci U S A 87:293–297. CrossRef Medline

Liebman PA, Parker KR, Dratz EA (1987) The molecular mechanism of visual excitation and its relation to the structure and composition of the rod outer segment. Annu Rev Physiol 49:765–791. CrossRef Medline

Ma J, Znoiko S, Othersen KL, Ryan JC, Das J, Isayama T, Kono M, Oprian DD, Corson DW, Cornwall MC, Cameron DA, Harosi FI, Makino CL, Crouch RK (2001) A visual pigment expressed in both rod and cone photoreceptors. Neuron 32:451–461. CrossRef Medline

Mou H, Cote RH (2001) The catalytic and GAF domains of the rod cGMP phosphodiesterase (PDE6) heterodimer are regulated by distinct regions of its inhibitory gamma subunit. J Biol Chem 276:27527–27534. CrossRef Medline

Muradov H, Boyd KK, Artemyev NO (2004) Structural determinants of the PDE6 GAF A domain for binding the inhibitory gamma-subunit and noncatalytic cGMP. Vision Res 44:2437–2444. CrossRef Medline

Muradov H, Boyd KK, Haeri M, Kerov V, Knox BE, Artemyev NO (2009) Characterization of human cone phosphodiesterase-6 ectopically expressed in *Xenopus laevis* rods. J Biol Chem 284:32662–32669. CrossRef Medline

Muradov H, Boyd KK, Artemyev NO (2010) Rod phosphodiesterase-6 PDE6A and PDE6B subunits are enzymatically equivalent. J Biol Chem 285:39828–39834. CrossRef Medline

Pang J, Boye SE, Lei B, Boye SL, Everhart D, Ryals R, Umino Y, Rohrer B, Alexander J, Li J, Dai X, Li Q, Chang B, Barlow R, Hauswirth WW (2010)

Self-complementary AAV-mediated gene therapy restores cone function and prevents cone degeneration in two models of Rpe65 deficiency. Gene Ther 17:815–826. CrossRef Medline

Pang JJ, Chang B, Kumar A, Nusinowitz S, Noorwez SM, Li J, Rani A, Foster TC, Chiodo VA, Doyle T, Li H, Malhotra R, Teusner JT, McDowell JH, Min SH, Li Q, Kaushal S, Hauswirth WW (2006) Gene therapy restores vision-dependent behavior as well as retinal structure and function in a mouse model of RPE65 Leber congenital amaurosis. Mol Ther 13:565–572. CrossRef Medline

Pang JJ, Lauramore A, Deng WT, Li Q, Doyle TJ, Chiodo V, Li J, Hauswirth WW (2008) Comparative analysis of in vivo and in vitro AAV vector transduction in the neonatal mouse retina: effects of serotype and site of administration. Vision Res 48:377–385. CrossRef Medline

Pang JJ, Dai X, Boye SE, Barone I, Boye SL, Mao S, Everhart D, Dinculescu A, Liu L, Umino Y, Lei B, Chang B, Barlow R, Strettoi E, Hauswirth WW (2011) Long-term retinal function and structure rescue using capsid mutant AAV8 vector in the rd10 mouse, a model of recessive retinitis pigmentosa. Mol Ther 19:234–242. CrossRef Medline

Prusky GT, Alam NM, Beekman S, Douglas RM (2004) Rapid quantification of adult and developing mouse spatial vision using a virtual optomotor system. Invest Ophthalmol Vis Sci 45:4611–4616. CrossRef Medline

Pugh EN Jr, Cobbs WH (1986) Visual transduction in vertebrate rods and cones: a tale of two transmitters, calcium and cyclic GMP. Vision Res 26:1613–1643. CrossRef Medline

Shi G, Yau KW, Chen J, Kefalov VJ (2007) Signaling properties of a short-wave cone visual pigment and its role in phototransduction. J Neurosci 27:10084–10093. CrossRef Medline

Shi GW, Chen J, Concepcion F, Motamedchaboki K, Marjoram P, Langen R, Chen J (2005) Light causes phosphorylation of nonactivated visual pigments in intact mouse rod photoreceptor cells. J Biol Chem 280:41184–41191. CrossRef Medline

Umino Y, Solessio E, Barlow RB (2008) Speed, spatial, and temporal tuning of rod and cone vision in mouse. J Neurosci 28:189–198. CrossRef Medline

Yamazaki A, Bartucca F, Ting A, Bitensky MW (1982) Reciprocal effects of an inhibitory factor on catalytic activity and noncatalytic cGMP binding sites of rod phosphodiesterase. Proc Natl Acad Sci U S A 79:3702–3706. CrossRef Medline

Zhang X, Wensel TG, Kraft TW (2003) GTPase regulators and photoresponses in cones of the eastern chipmunk. J Neurosci 23:1287–1297. Medline

Zhang XJ, Gao XZ, Yao W, Cote RH (2012) Functional mapping of interacting regions of the photoreceptor phosphodiesterase (PDE6) gamma-subunit with PDE6 catalytic dimer, transducin, and regulator of G-protein signaling9-1 (RGS9-1). J Biol Chem 287:26312–26320. CrossRef Medline

Zolotukhin S, Byrne BJ, Mason E, Zolotukhin I, Potter M, Chesnut K, Summerford C, Samulski RJ, Muzyczka N (1999) Recombinant adeno-associated virus purification using novel methods improves infectious titer and yield. Gene Ther 6:973–985. CrossRef Medline